inorganics

MDPI

Supplementary Materials: Copper(II) Complexes with Tetradentate Piperazine-Based Ligands: DNA Cleavage and Cytotoxicity

Sebastian Doniz Kettenmann [1], Yvonne Nossol [1], Febee R. Louka [2], Julia R. Legrande [2], Elise Marine [2], Roland C. Fischer [3], Franz A. Mautner [4], Vinja Hergl [1], Nora Kulak [1,5,*] and Salah S. Massoud [2,6,*]

Table of Contents

15) Figure S13. UV–VIS spectra of BNPP (270 μM) in MOPS buffer (10 mM, pH 7.4) in the presence of Cu(II) complexes (540 μM) after 2 h and 96 h incubation at 37 °C.

16) Figure S14**.** Changes of UV–VIS absorbance due to the cleavage of BNPP (270 μM) in MOPS buffer (10 mM, pH 7.4) in the presence of 540 μM Cu(II) complexes **2-ClO$_4$** (left) and **3-ClO$_4$** (right) after 2 h, 48 h, and 96 h incubation at 37 °C.

17) Figure S15. Fluorescence spectra of TPA and PBSF after incubation with/without [Cu(L^1)ClO$_4$]ClO$_4$ (**1-ClO$_4$**).

18) Figure S16**.** Results of the MTT assay (relative viability) in A2780 cells (a, c) and human fibroblasts (b, d) of Cu(II) complexes (a, b) and their ligands (c, d).

X-ray Crystallography of 4-Cl and 5-Cl

The X-ray single-crystal data of compounds **4-Cl** and **5-Cl** were collected on a Bruker-AXS APEX II CCD diffractometer at 100(2) K. The crystallographic data, conditions retained for the intensity data collection and some features of the structure refinements are listed in **Table S1**. The intensities were collected with Mo-Kα radiation (λ= 0.71073 Å). Data processing, Lorentz-polarization and absorption corrections were performed using SAINT, APEX and the SADABS computer programs [RS1]. The structures were solved by direct methods and refined by full-matrix least-squares methods on F^2, using the SHELXTL program package [RS2]. All non-hydrogen atoms were refined anisotropically. The hydrogen atoms were located from difference Fourier maps, assigned with isotropic displacement factors and included in the final refinement cycles by use of geometrical constraints. Molecular plots were performed with the MERCURY program [RS3]. Deposition numbers: CCDC-1919195 and CCDC-1919196 for **4-Cl** and **5-Cl**, respectively.

Table S1. Crystallographic data and processing parameters.

Compound	**4-Cl**	**5-Cl**
Empirical formula	$C_{20}H_{30}Cl_2CuN_4O_9$	$C_{22}H_{32}ClCuN_6F_6N_4O_2P_6$
Formula mass	604.93	628.49
System	Monoclinic	Monoclinic
Space group	$P2_1/n$	$P2_1/c$
a (Å)	14.0641(15)	11.7640(8)
b (Å)	7.3572(7)	15.6015(10)
c (Å)	24.751(3)	14.7695(11)
α (°)	90	90
β (°)	98.165(5)	99.030(4)
γ (°)	90	90
V (Å^3)	2535.1(5)	2677.1(3)
Z	4	4
T (K)	100(2)	100(2)
μ (mm^{-1})	1.129	1.045
D_{calc} (Mg/m^3)	1.585	1.559
θ max (°)	25.996	26.000
Data collected	84996	34462
Unique refl. / R_{int}	4965 / 0.0783	5058 / 0.0915
Parameters	330	381
Goodness-of-Fit on F^2	1.234	1.177
R1 / wR2 (all data)	0.0758 / 0.1676	0.0826 / 0.1916
Residual extrema (e/Å^3)	1.65 / -0.83	1.33 / -1.11
CCDC	1919195	1919196

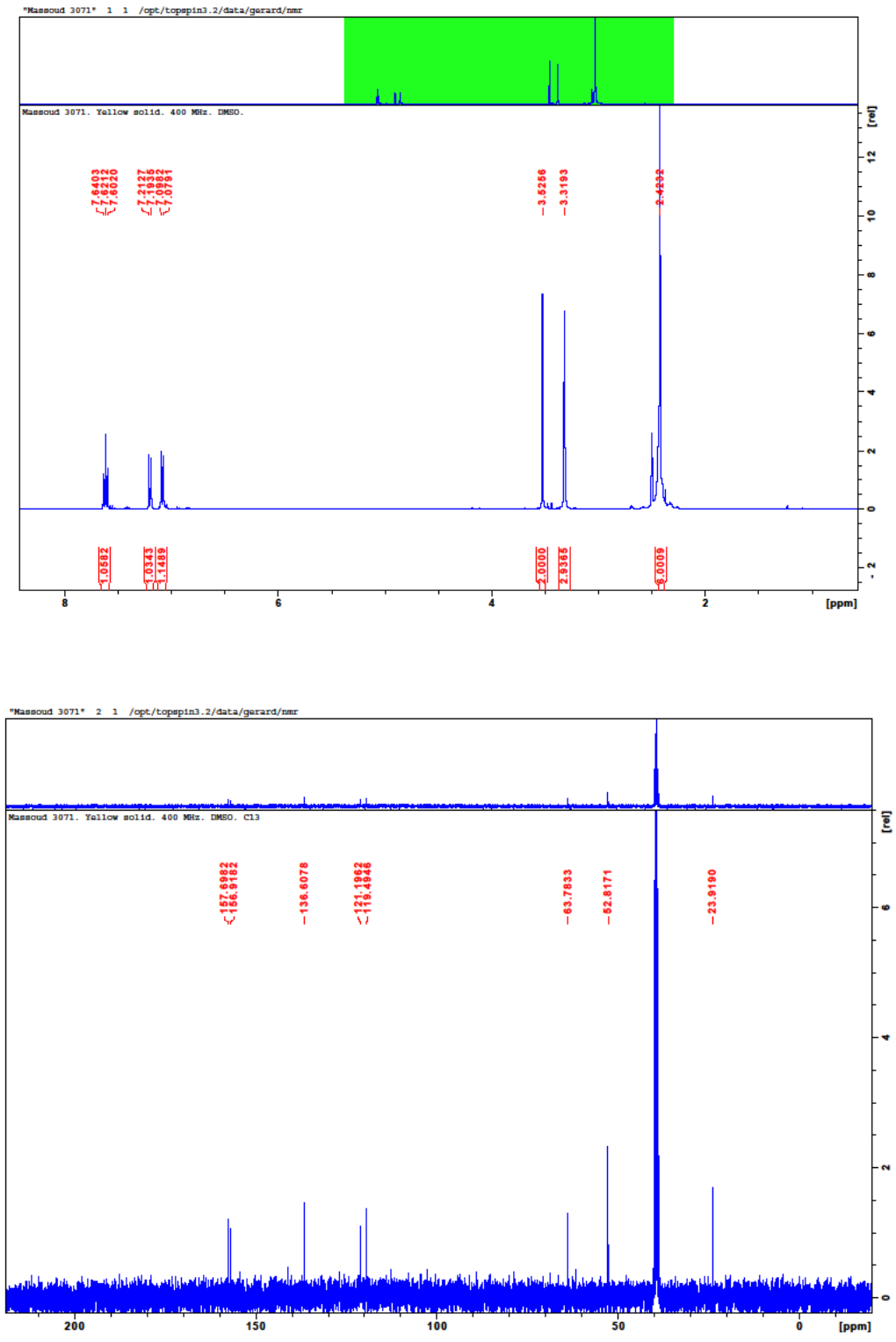

Figure S1. ^{1}H and ^{13}C NMR spectra of 1,4-bis[(6-methyl)-(2-pyridinyl)methyl]piperazine (L^2) in DMSO-d_6. .

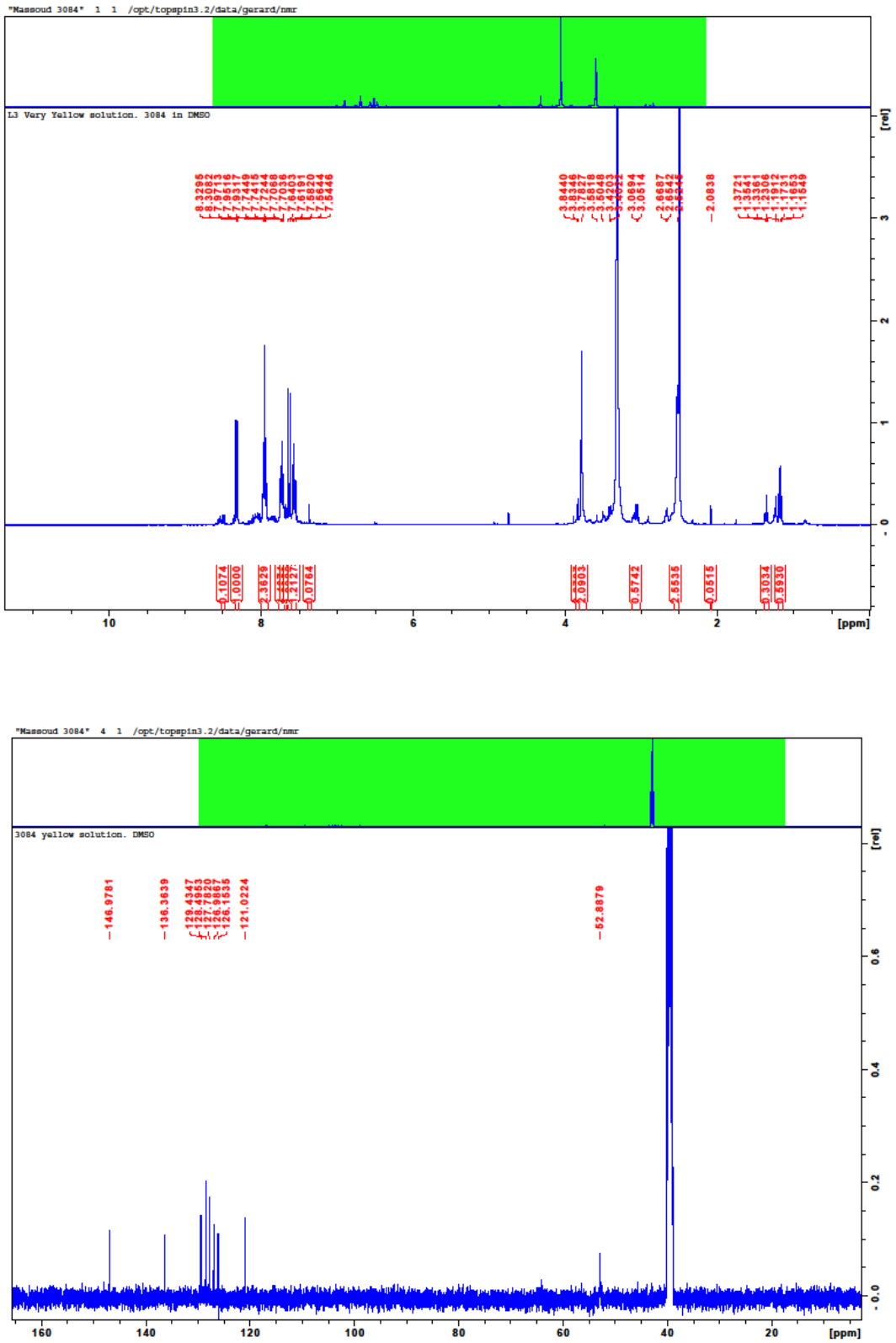

Figure S2. ^{1}H and ^{13}C NMR spectra of 1,4-bis[(2-quinolyl)methyl]piperazine (L^{3}) in DMSO-d_6.

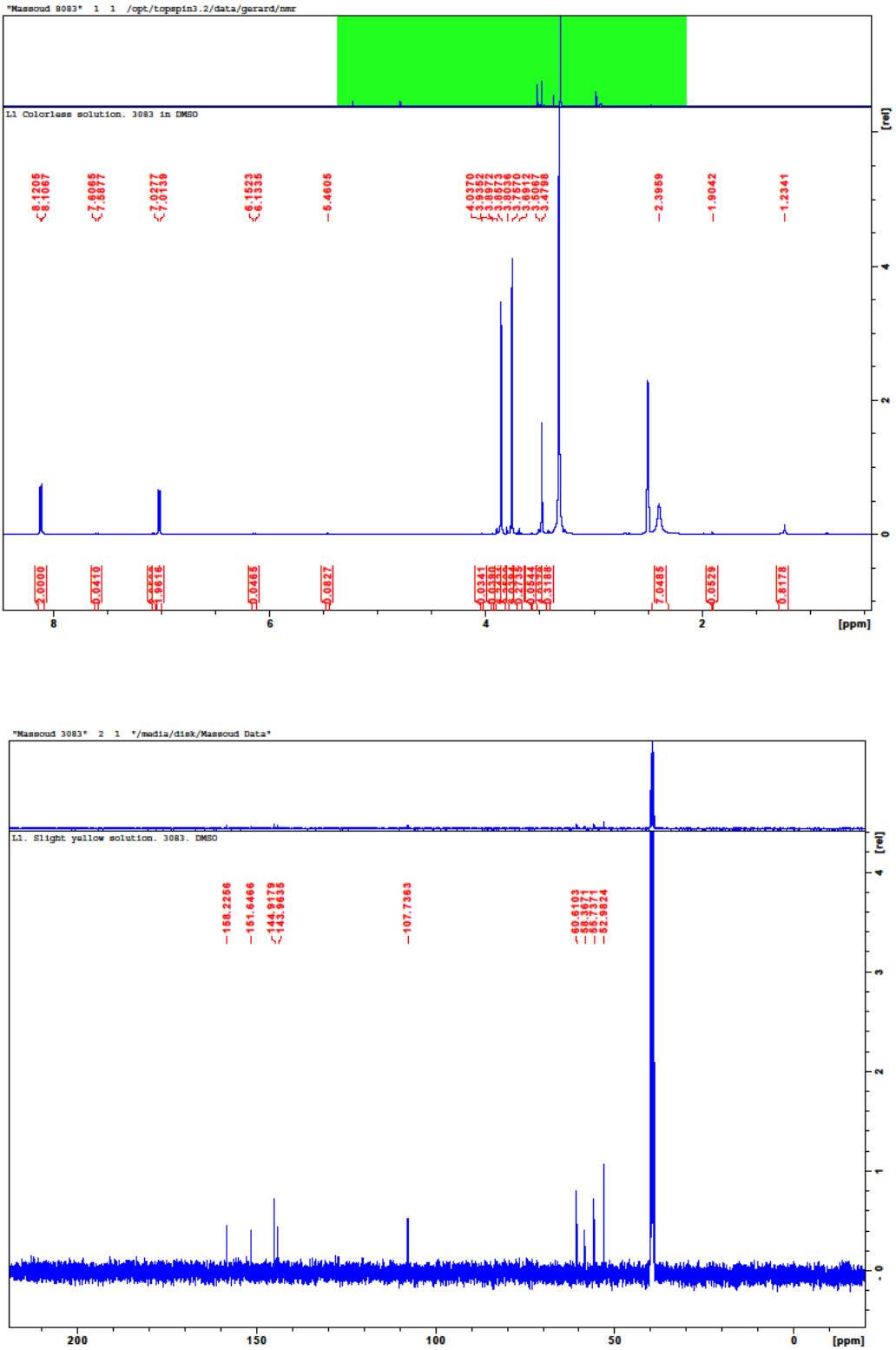

Figure S3. ^{1}H and ^{13}C NMR spectra of 1,4-bis[(3,4-dimethoxy-2-pyridinyl)methyl)]piperazine (L^4) in DMSO-*d*$_6$. .

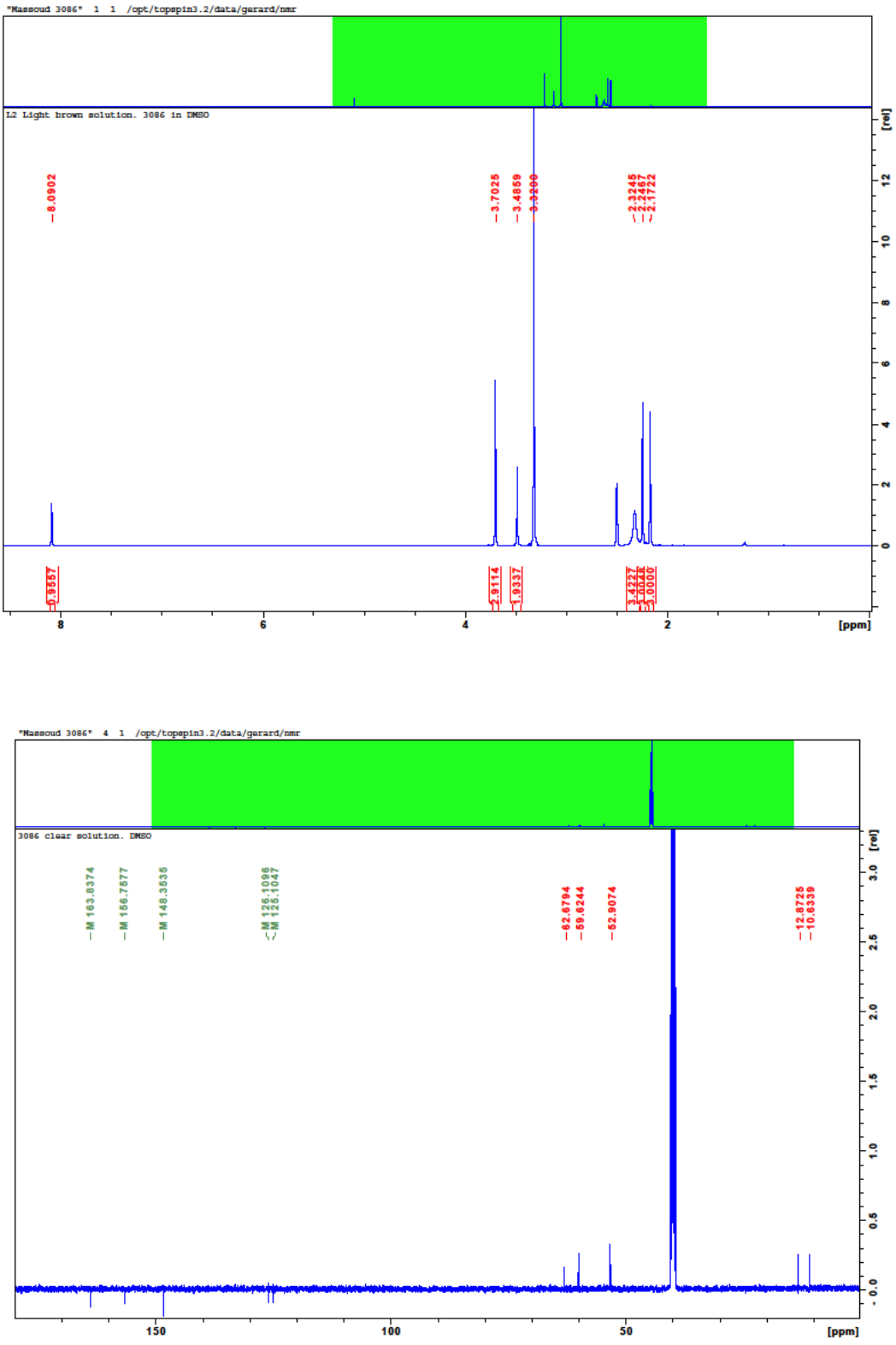

Figure S4. ^{1}H and ^{13}C NMR spectra of 1,4-bis[(3,5-dimethyl-4-methoxy-2-pyridinyl)methyl)]-piperazine (L^5) in DMSO-d_6.

.

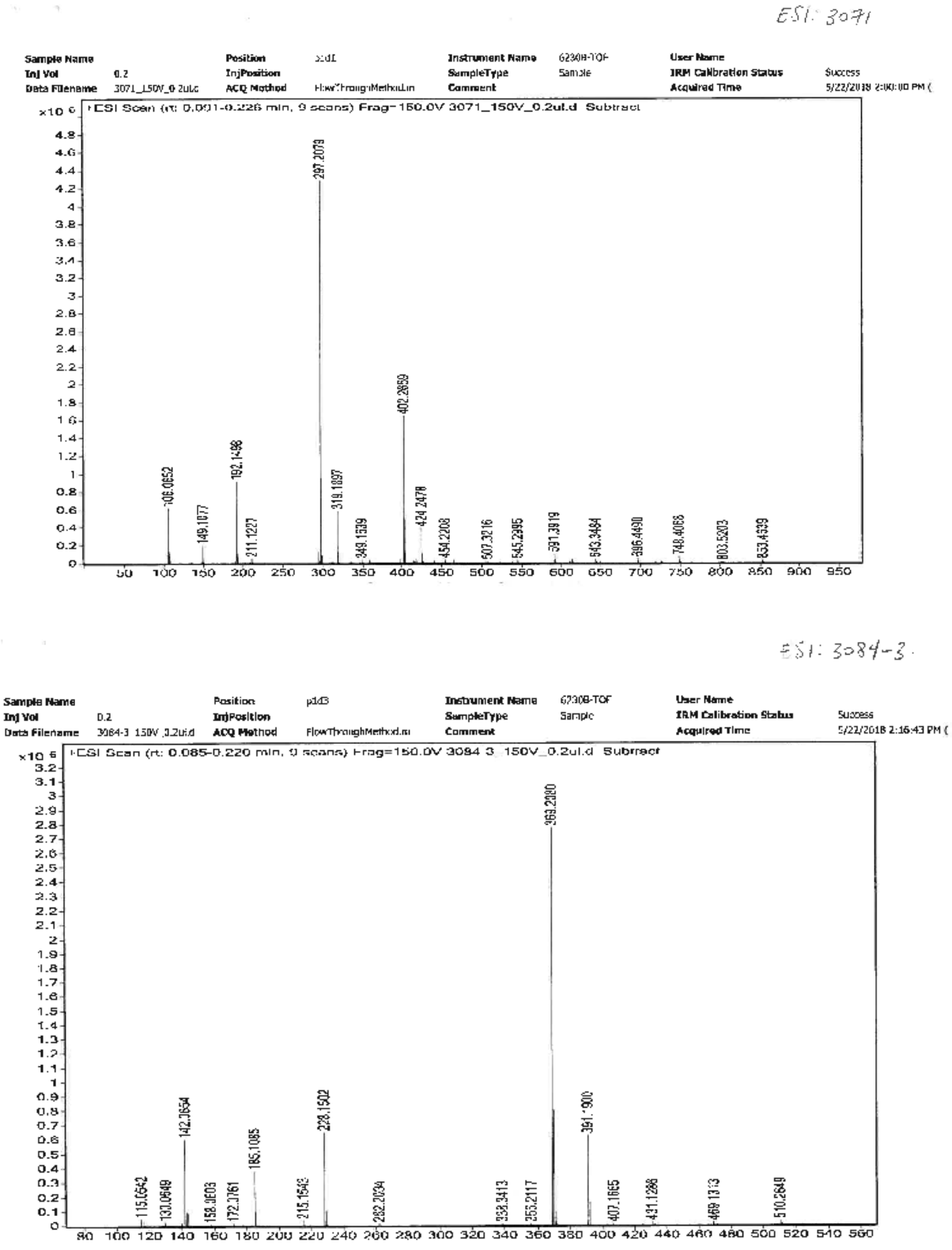

Figure S5. ESI-MS **of** 1,4-bis[(6-methyl)-(2-pyridinyl)methyl]piperazine (L^2) (top) and 1,4-bis[(2-quinolyl)methyl]piperazine (L^3) (bottom) in CH_3OH.

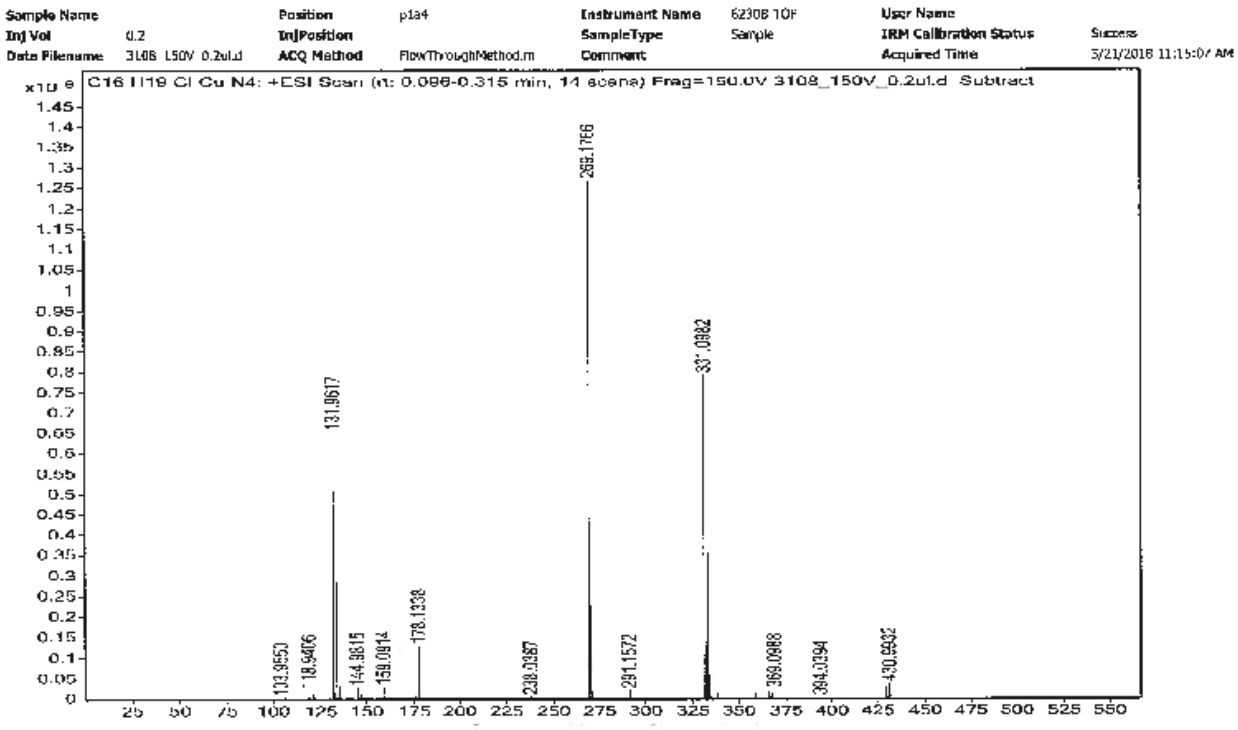

Figure S6. ESI-MS spectrum of **[Cu(L[1])Cl]PF$_6$** (**1-Cl**) in CH_3CN. .

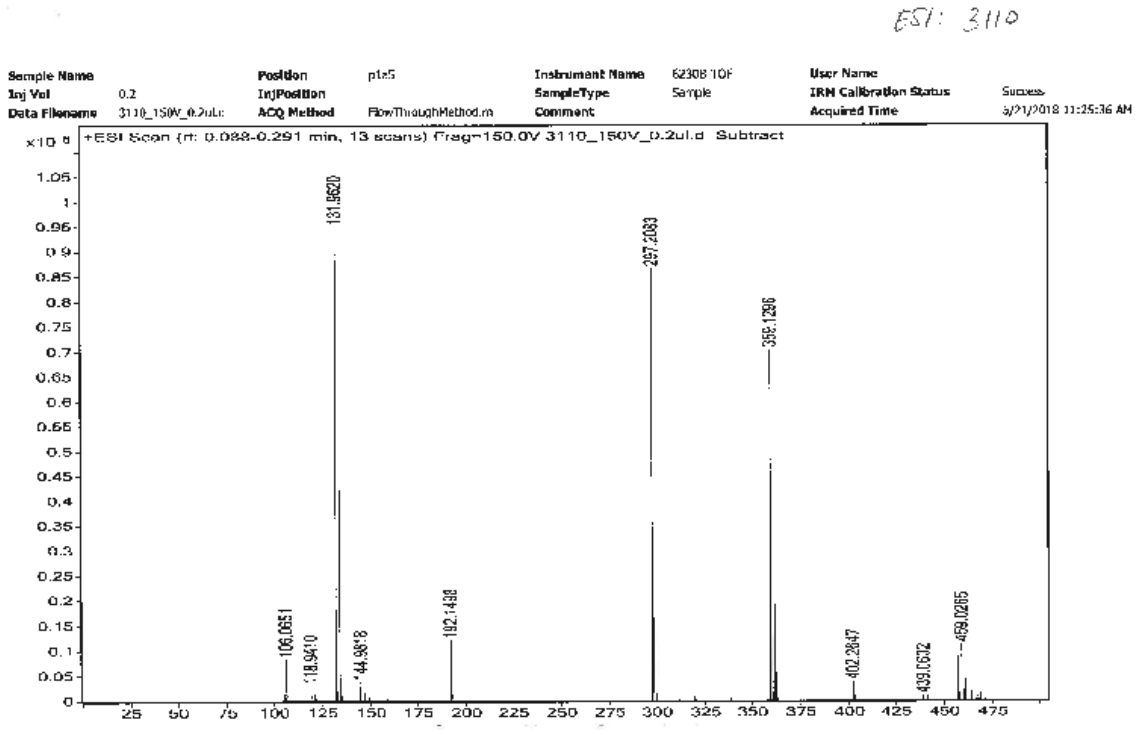

Figure S7. ESI-MS spectrum of $[Cu(L^2)ClO_4]ClO_4$ (**2-ClO$_4$**) in CH_3CN.

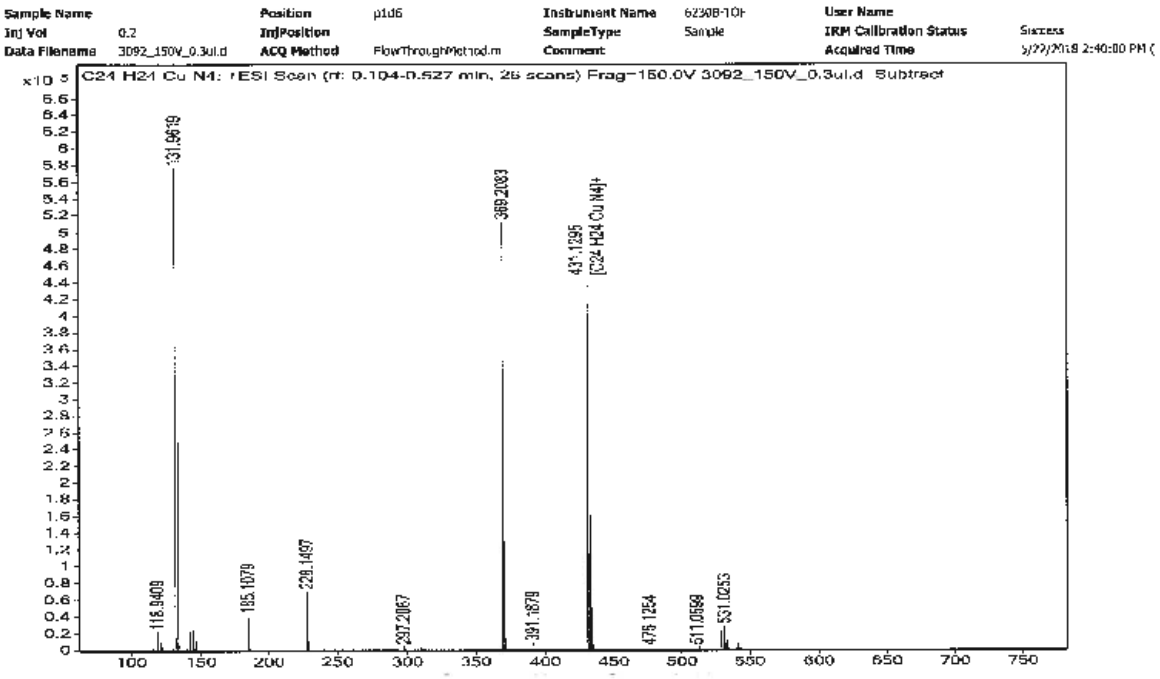

Figure S8. ESI-MS spectrum of $[Cu(L^3)ClO_4]ClO_4$ (**3-ClO$_4$**) in CH_3CN. .

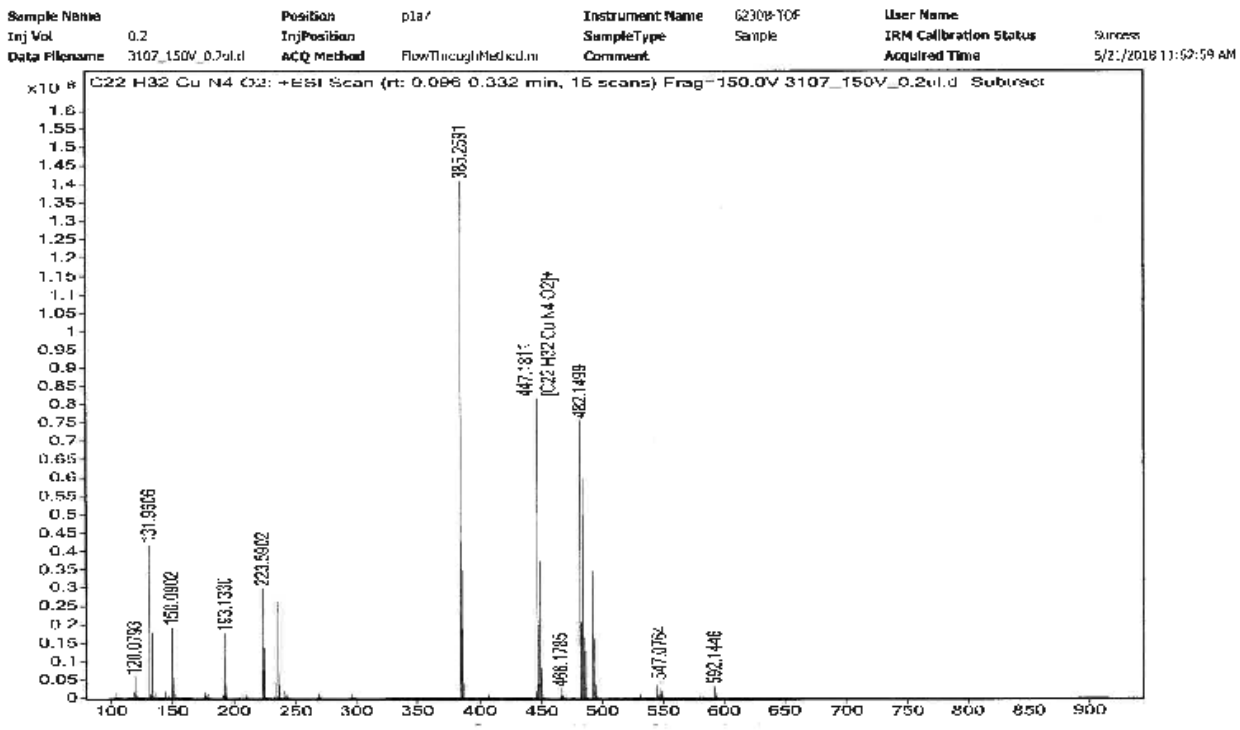

Figure S9. ESI-MS of $[Cu(L^5)Cl]PF_6$ (**5-Cl**) in CH_3CN.

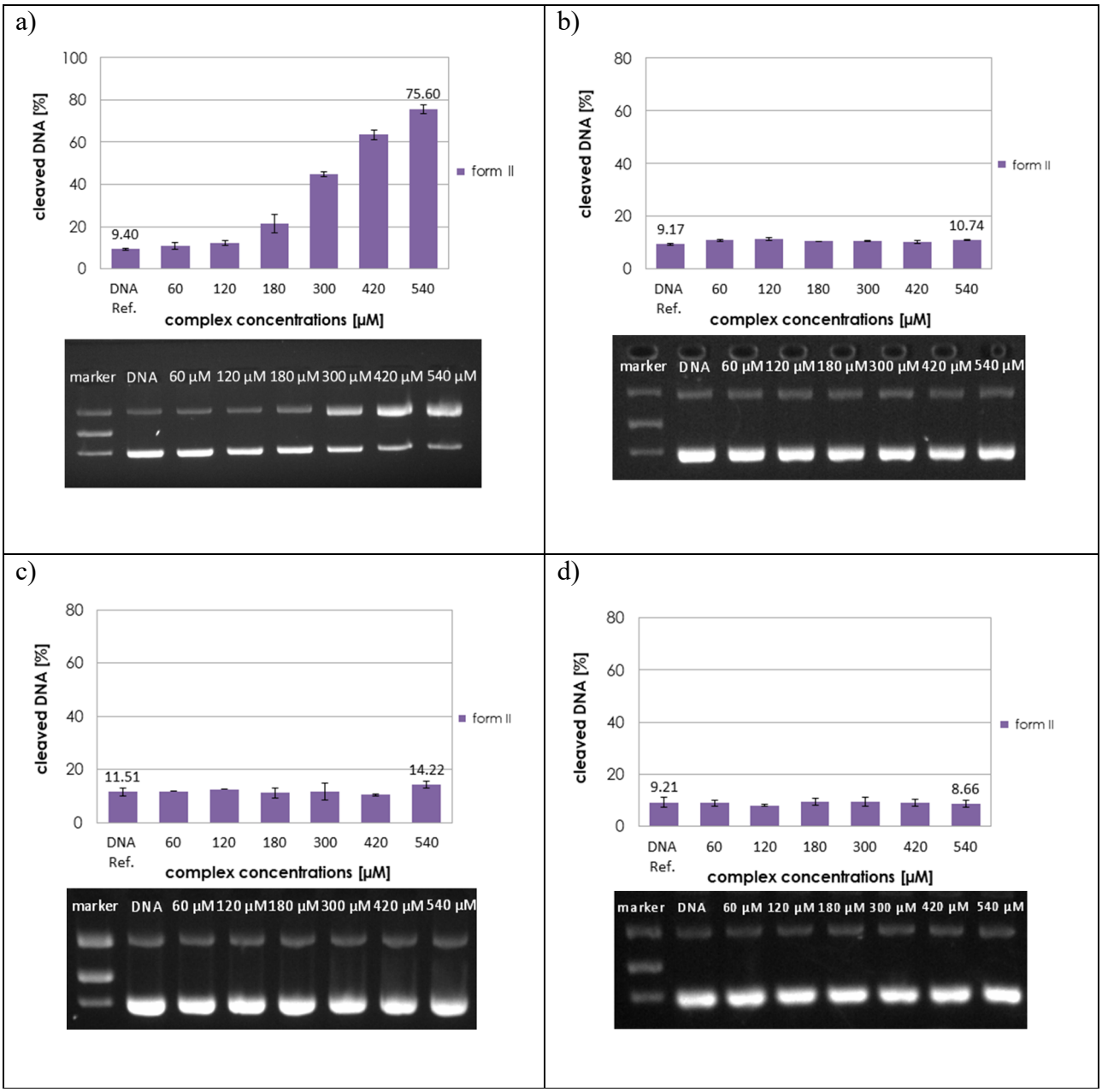

Figure S10. Cleavage of pBR322 plasmid DNA (0.025 µg/µL) into form **II** by complexes: a) **1-Cl**, b) **4-Cl**, c) **5-Cl**, and d) **6-ClO$_4$** at concentrations in the range of 60 to 540 µM after an incubation time of 2 h at pH 7.4 (10 mM MOPS) and 37 °C. Lane 1: Marker, Lane 2: control without added complex.

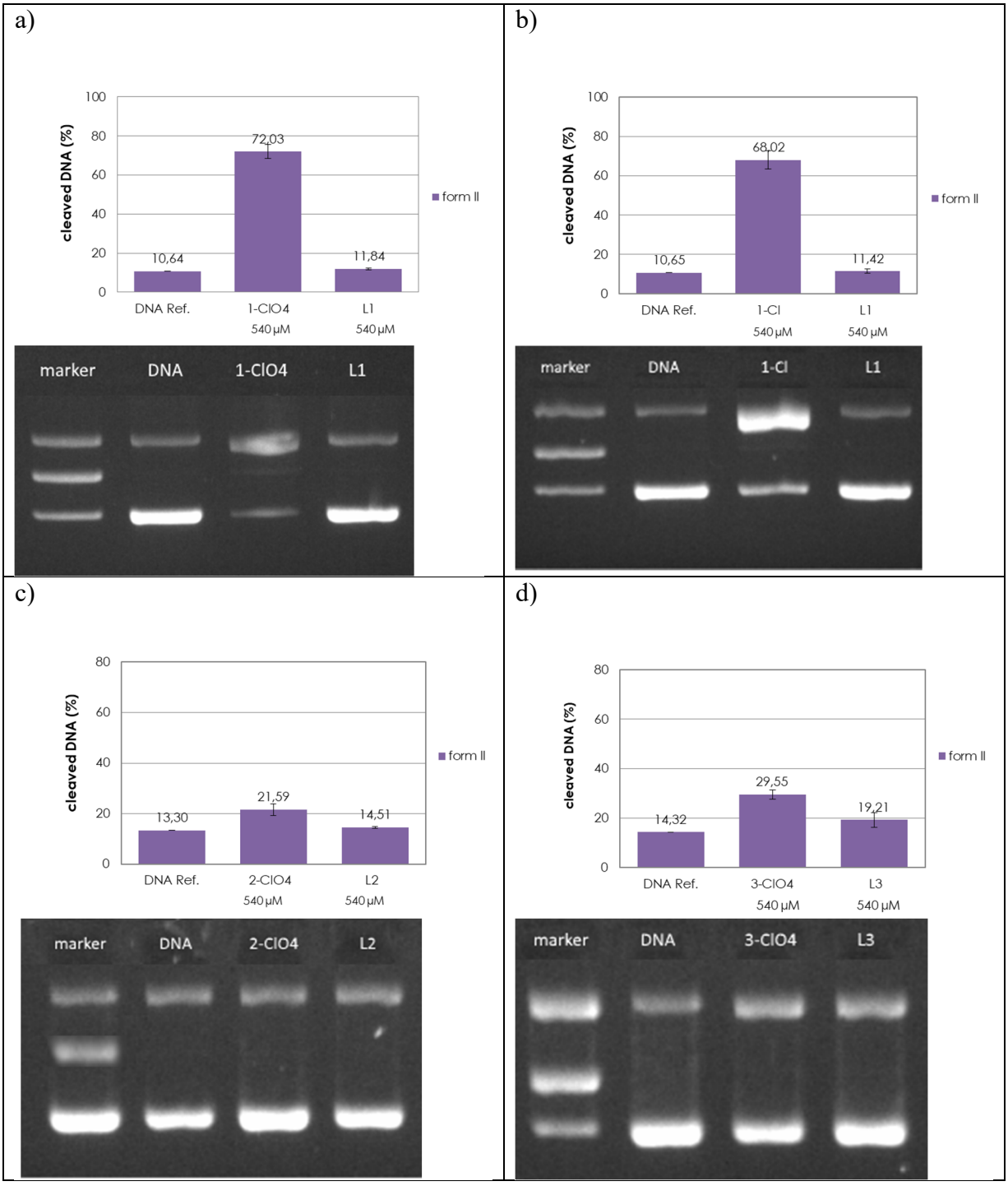
a)
cleaved DNA (%)
100
80
60
40
20
0
72,03
10,64
11,84
form II
DNA Ref.
1-ClO4
540 µM
L1
540 µM
marker
DNA
1-ClO4
L1
b)
cleaved DNA (%)
68,02
10,65
11,42
form II
DNA Ref.
1-Cl
540 µM
L1
540 µM
marker
DNA
1-Cl
L1
c)
cleaved DNA (%)
80
60
40
20
0
21,59
13,30
14,51
form II
DNA Ref.
2-ClO4
540 µM
L2
540 µM
marker
DNA
2-ClO4
L2
d)
cleaved DNA (%)
80
60
40
20
0
29,55
14,32
19,21
form II
DNA Ref.
3-ClO4
540 µM
L3
540 µM
marker
DNA
3-ClO4
L3

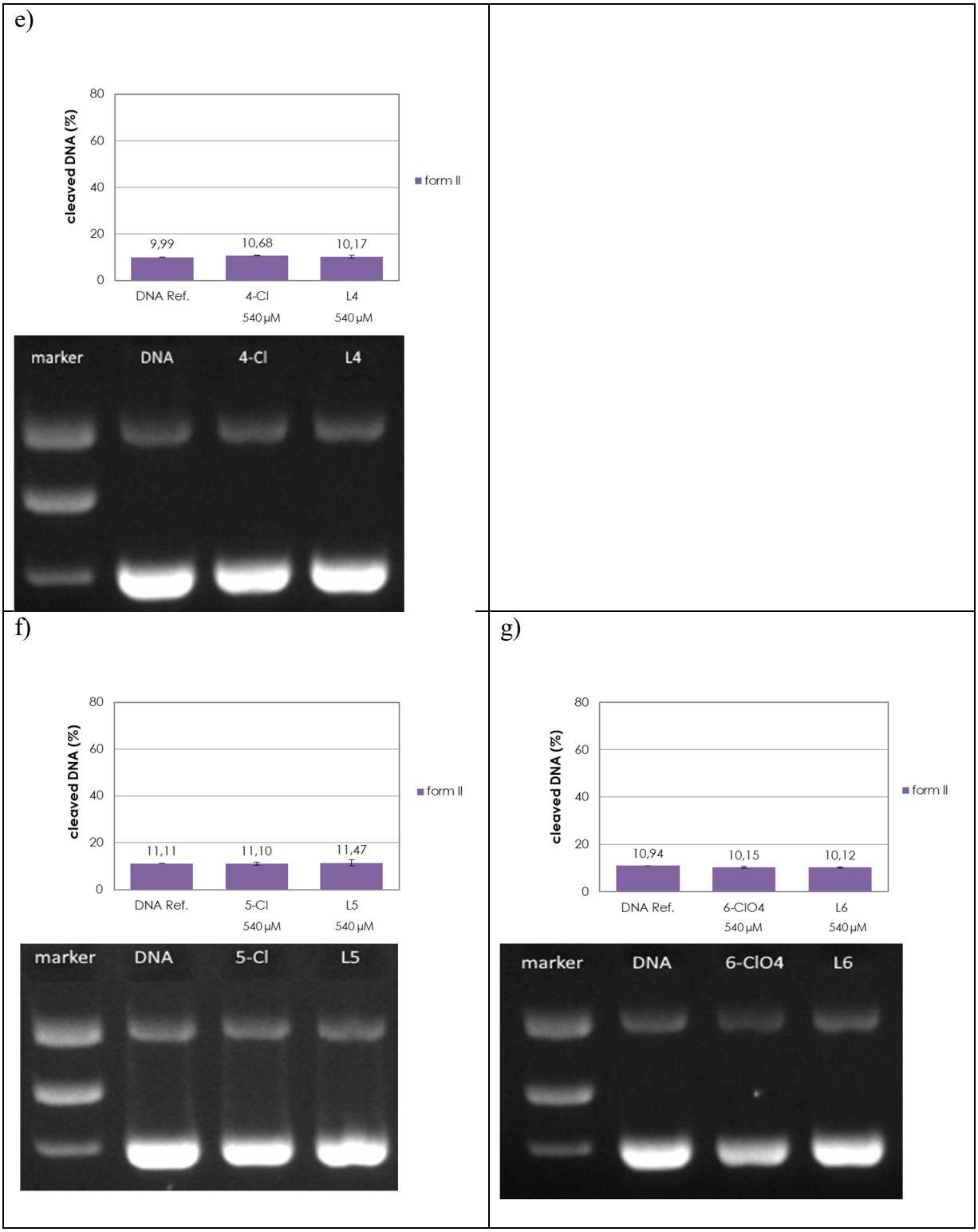

Figure S11. Cleavage of pBR322 plasmid DNA (0.025 µg/µL) by complexes and the respective ligands: a) **1-ClO$_4$** and L^1, b) **1-Cl** and L^1, c) **2-ClO$_4$** and L^2, d) **3-ClO$_4$** and L^3, e) **4-Cl** and L^4, f) **5-Cl** and L^5, g) **6-ClO$_4$** and L^6 at a concentration of 540 µM after an incubation time of 2 h at pH 7.4 (10 mM MOPS) and 37 °C. Lane 1: Marker, Lane 2: control without added complex/ligand.

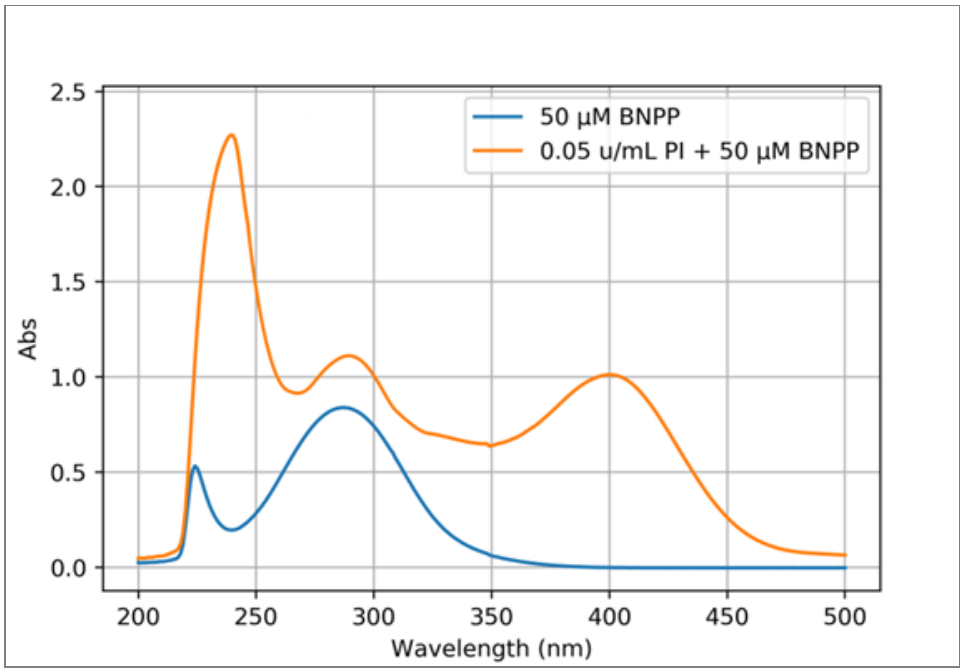

Figure S12. UV–VIS spectra of BNPP (50 µM) in MOPS buffer (10 mM, pH 7.4) in the absence and presence of phosphodiesterase (PI, 0.05 u/mL) after 2 h incubation.

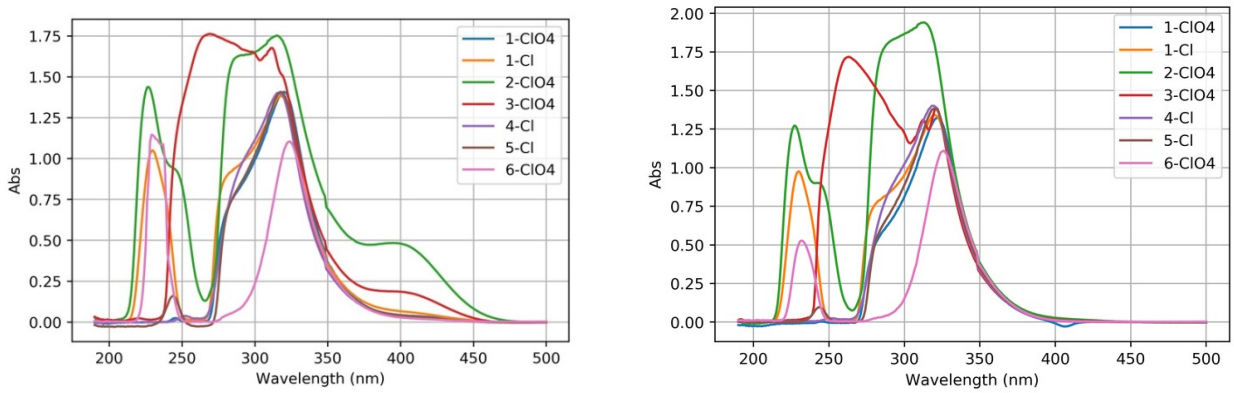

FigureS 13. UV–VIS spectra of BNPP (270 µM) in MOPS buffer (10 mM, pH 7.4) in the presence of Cu(II) complexes (540 µM) after 2 h (left) and 96 h (right) h incubation at 37 °C.

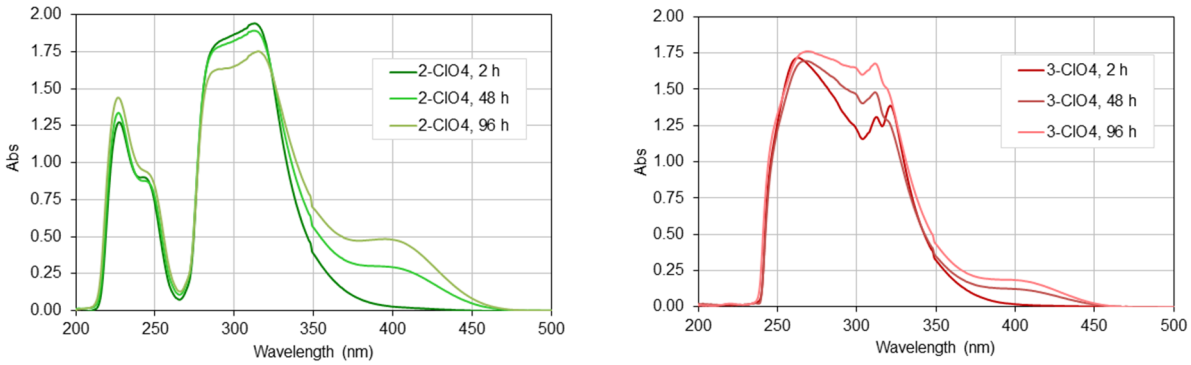

Figure S14. Changes of UV–VIS absorbance due to the cleavage of BNPP (270 μM) in MOPS buffer (10 mM, pH 7.4) in the presence of 540 μM Cu(II) complexes **2-ClO$_4$** (left) and **3-ClO$_4$** (right) after 2 h, 48 h, and 96 h incubation at 37 °C.

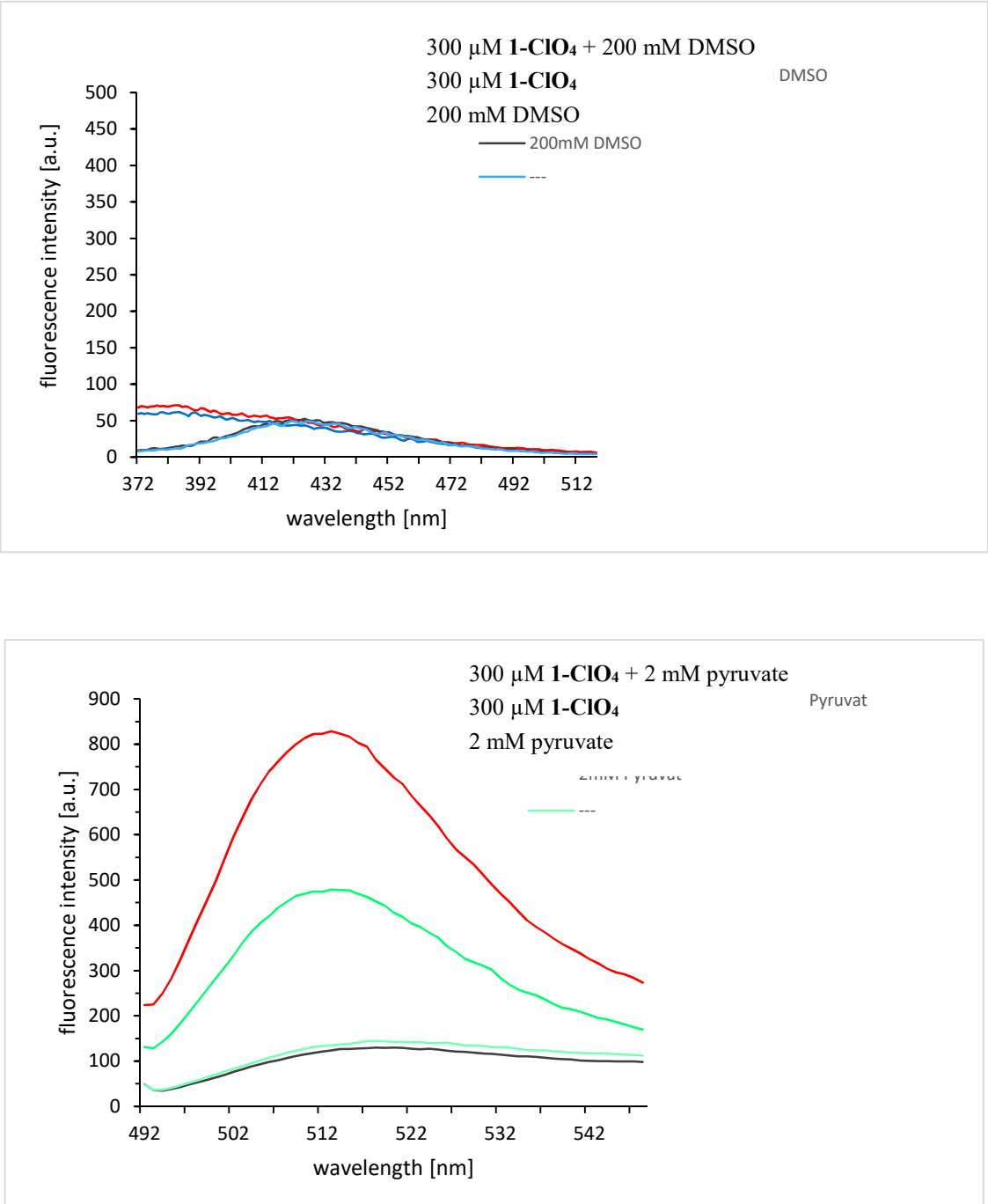

Figure S15. Fluorescence spectra of TPA (terephthalic acid, above) and PBSF (pentafluorobenzenesulfonyl fluorescein, below) after incubation with/without [Cu(L[1])ClO4]ClO4 (**1-ClO4**) and with/without quenchers DMSO and pyruvate, respectively. As a control, the fluorogenic compounds are also, shown alone in the presence and absence of the respective quencher. The experiments were carried out following a previously published protocol [ref. 54 in the manuscript], however, without the addition of ascorbate as a reductant.

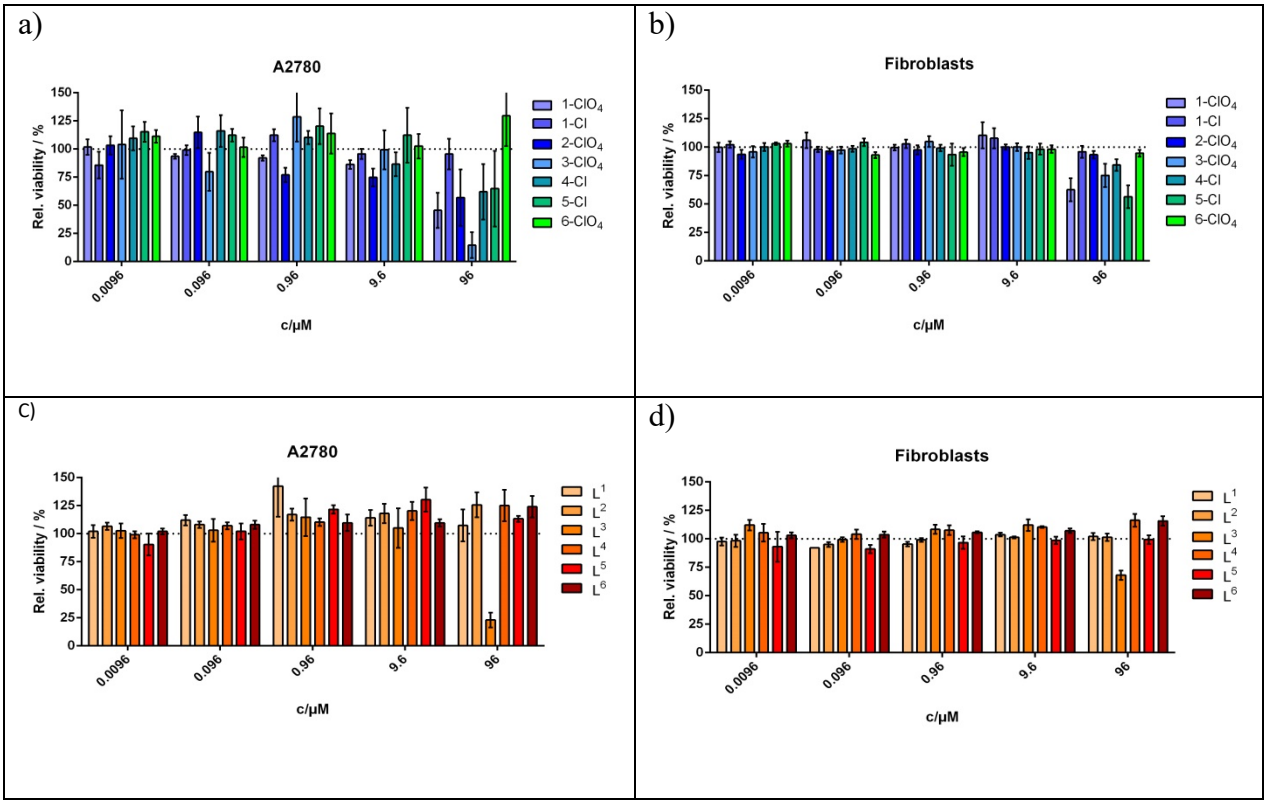

Figure S16. Results of the MTT assay (relative viability) in A2780 cells (a, c) and human fibroblasts (b, d) of Cu(II) complexes (a, b) and their ligands (c, d). Concentrations of 0.0096, 0.096, 0.96, 9.6, 96 and 115 µM compound were incubated with the respective cells for 48 h at 37 °C.

References

[RS1] Bruker (2005) SAINT v. 7.23; Bruker (2006) APEX 2v. 2.0-2; Bruker AXS Inc. Madison, Wisconsin, USA; b) G. M. Sheldrick (2001), SADABS v. 2. University of Goettingen, Germany.

[RS2] G. M. Sheldrick, *Acta Crystallogr.* **2008**, A64, 112.

[RS3] C. F. Macrae, P. R. Edington, P. McCabe, E. Pidcock, G. P. Shields, R. Taylor, T. Towler, J. van de Streek, *J. Appl. Crystallogr.* **2006**, 39, 453.